International Journal of Modern Physics D
Vol. 25, No. 1 (2016) 1650003 (18 pages)

DOI: 10.1142/S0218271816500036

World Scientific
www.worldscientific.com

Constraints on interacting dark energy from time delay lenses

Yu Pan

College of Science,
Chongqing University of Posts and Telecommunications,
Chongqing 400065, P. R. China

State Key Laboratory of Theoretical Physics,
Institute of Theoretical Physics,
Chinese Academy of Sciences, Beijing 100190, P. R. China

Shuo Cao*

Department of Astronomy, Beijing Normal University,
Beijing 100875, P. R. China
caoshuo@bnu.edu.cn

Li Li

College of Science,
Chongqing University of Posts and Telecommunications,
Chongqing 400065, P. R. China

Received 29 May 2015
Revised 29 July 2015
Accepted 27 August 2015
Published 1 October 2015

We use the time delay measurements between multiple images of lensed sources in 18 strongly gravitationally lensed (SGL) systems to put additional constraints on three phenomenological interaction models for dark energy (DE) and dark matter (DM). The compatibility among the fits on the three models seems to imply that the coupling between DE and DM is a small value close to zero, which is compatible with the previous results for constraining interacting DE parameters. We find that, among the three interacting DE models, the γ_mIDE model with the interaction term Q proportional to the energy density of DM provides relatively better fits to recent observations. However, the coincidence problem is still very severe in the framework of three interacting DE models, since the fitting results do not show any preference for a nonzero coupling between DE and DM. More importantly, we have studied the significance of the current strong lensing data in deriving the interacting information between dark sectors,

*Corresponding author.

which highlights the importance of strong lensing time delay measurements to provide additional observational fits on alternative cosmological models.

Keywords: Cosmological parameters — (Cosmology:) dark energy; Gravitational lensing: strong.

PACS Number(s): 95.36.+X, 98.80.Es

1. Introduction

As one of the successful predictions of general relativity, the discovery of the lensed quasar system Q0957+561,[1] has opened up an interesting possibility to use strong lensing systems in the study of cosmology and astrophysics. Strong gravitational lensing, which reveals itself as multiple images of the source, occurs whenever the source, the lens and the observer are so well aligned that the observer-source direction lies inside the so-called Einstein ring of the lens. Moreover, the image separation in the system depends on angular diameter distances to the lens and to the source, which in turn could perform an important astrophysical tool for probing the background cosmology.[2–9]

In addition, multiple images of the lensed variable sources take different time to complete their travel. Time delays between the various images of the background source Δt are directly related to the potential of the deflector as well as the geometry of the universe through

$$\Delta t \propto D_{\Delta t} \Delta\phi, \tag{1}$$

where $\Delta\phi$ is Fermat potential containing all of the dependence on the mass distribution, and $D_{\Delta t}$ is the so-called time delay distance (TDD) depending only on the background cosmological expansion. The bending of light by a gravitational body was predicted by Einstein (1912),[10] a few years before the publication of general relativity. General discussion of the geodesic deviation equations as the underlying physical description of image distortion could be found in many standard references.[11] The idea of using gravitational lenses with time delays between the various images of a background quasar as a cosmological probe was firstly initiated by Refsdal[12] and then developed successfully to test modern competing cosmologies. Based on the expected numbers of lenses and relevant uncertainties calculated for Pan-STARRS 1, LSST, and OMEGA, Coe and Moustakas[13] explored the great potential of gravitational lens time delays to constrain cosmological parameters (H_0, Ω_m, w). As of today, time delays have been observed from 21 lensed quasars but this is only the beginning. In the near future, this sample will be enlarged to 1000s of systems by various observational programmes, such as LSST, the COSmological MOnitoring of GRAvitational Lenses (COSMOGRAIL),[15] the International Liquid Mirror Telescope (ILMT) project,[16] and the dark energy (DE) survey.[17–19]

More recently, the measurements of TDD between multiple images of lensed sources ($D_{\Delta t}$) have become an effective probe in cosmology, which was proposed to test the cosmological parameters including Hubble constant and the properties of DE.[20–23] By combining the improved TDD measurements of gravitational lens RXJ1131-1231 with the WMAP9 and Planck posteriors, Suyu *et al.*[14] obtained $\Omega_k = 0.00^{+0.01}_{-0.02}$ in an open ΛCDM model and $w = -1.52^{+0.19}_{-0.20}$ in a flat wCDM model.[14] In this paper, we mainly focus on the constraint on the interaction between DE and dark matter (DM), based on the newest observations of TDD for 18 strong lensing systems compiled by Mauro *et al.*[23] They developed a method to measure the Hubble constant and to characterize the DE based on free-form modeling and apply it to time delay measurements already available. Similar approaches were successfully used in the past to constrain H_0 under the assumption that DM density and DE were known.[24–26] With 18 systems having time delay measurements, Mauro *et al.*[23] obtained a reasonable fit on the Hubble constant $H_0 = 69 \pm 6\,\mathrm{km\,s^{-1}\,Mpc^{-1}}$.[23] The idea of using such systems was also discussed in Wei *et al.*,[27] which used 12 lens systems to optimize the parameters of $R_h = ct$ cosmology and make comparisons with the standard ΛCDM model. In this paper, we will broaden the application of this new, important cosmic probe by using the newly compiled data set to make constraints and carry out comparisons between competing interacting DE models.

In fact, DE is one of the most important issues in modern cosmology, since many astrophysical and cosmological observations such as Type Ia Supernovae (SN)[28–31] and cosmic microwave background radiation (CMB)[32–35] have indicated that the universe is undergoing an accelerated expansion at the present stage. The simplest candidate for these uniformly distributed DE is considered to be in the form of vacuum energy density or cosmological constant (Λ). However, the simple cosmological constant is always entangled with the coincidence problem: The matter density ρ_m decreases with the expansion of our universe with a^{-3} and the density of cosmological constant ρ_Λ does not change with the expansion of the universe, whereas the DE density is comparable with the dark energy density today. It is natural to consider the possibility of exchanging energy between DE and DM through an interaction term, as the coupling between DE and DM can provide a mechanism to alleviate the coincidence problem.[36–40] The idea of considering interaction between DM and a scalar field with negative pressure called "quintessence" was firstly proposed by Wetterich,[36] and well developed by Zimdahl *et al.*[37] As another phenomenological solution of the coincidence problem, interacting quintessence might lead to a constant ratio of the energy densities of DE and pressureless cold dark matter (CDM) fluid.[37] Considering the linear and nonlinear interactions depending on the DM and DE densities, Bolotin *et al.*[38] studied the cosmological evolution with interaction between DE and DM, and found that the interaction dynamics of a universe can differ significantly from the standard cosmological model.[38] Furthermore, it has been argued that an appropriate interaction between DE and DM can influence the

perturbation dynamics and affect the lowest multipoles of the CMB spectrum.[41,42] Recently, it has been shown that such an interaction could be inferred from the expansion history of the universe, as manifested in the supernova data together with CMB and large-scale structure.[43] However, the observational limits on the strength of such an interaction remain weak.[44] Signature of the interaction between DE and DM in the dynamics of galaxy clusters has also been analyzed.[45]

However, since neither DE nor DM is actually known to us, it is hard to describe the interaction from first principles. Some attempts to discriminate the interaction from the thermodynamical point of view have been raised recently,[46–48] in which most of the studies on the interaction between dark sectors rely either on the assumption of interacting fields from the outset or from phenomenological requirements. As extensively considered in the literature,[46,49–54] we assume that DE and dust matter exchange energy through an interaction term Q,

$$\begin{aligned} \dot{\rho}_x + 3H(\rho_x + p_x) &= -Q, \\ \dot{\rho}_m + 3H\rho_m &= Q, \end{aligned} \tag{2}$$

which preserves the total energy conservation equation $\dot{\rho}_{\rm tot} + 3H(\rho_{\rm tot} + p_{\rm tot}) = 0$. If Q is a nonzero function of the scale factor, the interaction makes ρ_m and ρ_x to deviate from the standard scaling.

The interacting DE models we consider in this paper were extensively discussed under the constraint of various astronomical observations, such that SNIa and from the history of the Hubble parameter.[54,55] In this paper, we use strongly gravitationally lensed (SGL) systems, to provide additional constraints on these interacting DE models. Using SGL features we compare three cases of interacting DE models, and study the relation between the energy density ratio of DM and DE and the equation-of-state (EoS) parameter in these cases. An interesting result of this study is that the role of potential interactions in the dark sector could be clarified. It is noteworthy that any interaction model introduces relations between the matter content and the EoS of dark energy.

To reduce the uncertainty and put tighter constraint on the value of the coupling, and examine the role of the $D_{\Delta t}$ data played in cosmological constraints, we also add other recent astrophysical observations, including the CMB observation from the Planck results,[56,57] and the BAO distance ratio (d_z) data[58–60] in our discussion. We expect that sensitivities of measurements of different observables can give complementary results on the coupling between dark sectors. Moreover, in order to make a comparison for various DE models and decide on the model preferred by the current data, we also apply a model comparison statistic, i.e. the information criterion in our analysis.

This paper is organized as follows. We introduce the observational data including the TDDs for 18 strong lensing systems in Sec. 2. In Sec. 3, we perform a Markov chain Monte Carlo constraint on three interacting dark energy models. In Sec. 4, theoretical analysis of the constraint results is presented and discussed. Finally, we summarize the main conclusions in Sec. 5.

2. Time Delay Distance Data and Other Observations

For a source located at the position β, the time delay between two images at positions θ_i and θ_j can be expressed as

$$\tau(\theta_{\mathbf{i}}) - \tau(\theta_{\mathbf{j}}) = \frac{\mathbf{c\Delta t_{ij}}}{\mathbf{D_{\Delta t}}}, \tag{3}$$

where τ represents the dimensionless arrival time, which depends on the properties of lenses

$$\tau(\theta) = \frac{\mathbf{1}}{\mathbf{2}}|\theta|^{\mathbf{2}} - \theta \cdot \beta, \tag{4}$$

and Δt_{ij} is the measured value of time delay. $D_{\Delta t}$ indicates the TDD defined as

$$D_{\Delta t} = (1 + z_d)\frac{D_d D_s}{D_{ds}}, \tag{5}$$

where D_d is the angular diameter distance from the observer to the lens at redshift z_d, D_s is the angular diameter distance from the observer to the source at redshift z_s, and D_{ds} is the angular diameter distance from the lens to the source. It is obvious that the TDD depends only on the cosmological models and therefore relevant cosmological parameters.

Usually, time delays of strong gravitational lenses is not straightforward measurement because of the lens mass distribution and the possible presence of other perturbing masses along the line of sight. To solve this point, three main methods have been employed to model the lens itself. One uses simply-parametrized forms for the mass distribution of the deflector called simple parametric method,[61] one uses as parameters a grid of pixels to describe either the potential or the mass distribution of the deflector and the source surface brightness distribution called grid-based parametric approach,[25,62–64] and the third method is a hybrid approach, in which pixelated corrections were made to a simply parametrized mass model.[65,66]

Recently, Saha *et al.*[67] developed a code called PixeLens to reconstruct a pixelated lens mass map by generating a large ensemble of models, which has been successfully applied to observational data.[23–26,67,68] More recently, Mauro *et al.*[23] proposed a new method of free-form modeling of gravitational lenses with the PixeLens formalism,[23] which successfully avoids the degeneracy between cosmological parameters the steepness of the lens mass profile. By applying this novel method to 18 systems having time delay observations, they obtained the TDD measurement for each lensing system, which will be used in our analysis.

The 18 lenses with measured time delays consist the following systems: 11 double lenses (Number of images $N_{\rm img} = 2$) (JVAS B0218+357, FBQS J0951+2635, HE 1104−1805, SBS 1520+530, CLASS B1600+434, HE 2149−2745;[69] SBS 0909+532,[70,71] Q J0957+561,[72] SDSS J1206+4332,[73] SBS J1650+4251,[74] PKS 1830−211[75]) and 7 quadruply lenses ($N_{\rm img} = 4$) (RX J0911+0551, PG 1115+080, CLASS B1608+656;[69] SDSS J1004+4112,[76] RX J1131−1231,[77] WFI J2033−4723,[78] HE 0435−1223[79]). We remark here that, due to the uncertain time

delay uncertainty and lacking spectroscopic measurements of z_d, several lensing systems with time delay measurements (B 1422+231, HS 2209+1914, H 1413+117 and SDSS J1029+2623) are excluded from the final sample. Following the method proposed in Mauro *et al.*,[23] for the main lenses of doubly imaged quasars, the mass distribution was required to have 180° rotation symmetry, while lenses with irregular quadruply imaged systems were modeled as asymmetric distribution. Meanwhile, for the systems showing evidence of external distortion, a constant external shear was added to contribute to the lensing. Finally, extra visible lenses, i.e. galaxies visible in the field with redshift similar to the main lens, were modeled as point masses at the corresponding pixel location.[a] The inclusion of extra lenses may effectively break the global 180° rotation symmetry.[26]

Full information about the TDDs data may be found in Table 2 of Mauro *et al.*[23] To constrain the cosmological parameters, we will perform a standard Bayesian analysis by minimizing χ^2,

$$\chi^2_{D_{\Delta t}} = \sum_{i=1}^{18} \frac{[D^{\rm th}_{\Delta t}(i) - D^{\rm obs}_{\Delta t}(i)]^2}{\sigma(i)^2}, \tag{6}$$

where $D^{\rm th}_{\Delta t}$ is the predicted time distance value in the cosmological model and $D^{\rm obs}_{\Delta t}$ is the measured value with a uncertainty of $\sigma(i)$.

In order to break the degeneracy of model parameters, we combine the $D_{\Delta t}$ data with the CMB observation from the Planck results[56,57] and the BAO observation.[58–60] We also add the Union2.1 set which consists of 580 SN Ia[80] to examine the role of the $D_{\Delta t}$ data played in cosmological constraints.

For CMB, we use the derived data set from the planck measurement, including the acoustic scale l_a, the shift parameter R, and baryonic matter fraction $\Omega_b h^2$[56,57]

$$\bar{\mathbf{P}}_{\rm CMB} = \begin{pmatrix} \bar{l}_a \\ \bar{R} \\ \bar{\Omega}_b h^2 \end{pmatrix} = \begin{pmatrix} 301.57 \pm 0.18 \\ 1.7407 \pm 0.0094 \\ 0.02228 \pm 0.0003 \end{pmatrix}. \tag{7}$$

The χ^2 value of the CMB observation can be expressed as[81]

$$\chi^2_{\rm CMB} = \Delta\mathbf{P}^{\rm T}_{\rm CMB}{\mathbf{C}_{\rm CMB}}^{-1}\Delta\mathbf{P}_{\rm CMB}, \tag{8}$$

where $\Delta\mathbf{P}_{\rm CMB} = \mathbf{P}_{\rm CMB} - \bar{\mathbf{P}}_{\rm CMB}$, and the corresponding inverse covariance matrix is

$${\mathbf{C}_{\rm CMB}}^{-1} = \begin{pmatrix} 43.018 & -366.7718 & 2972.5 \\ -366.7718 & 24873 & 446500 \\ 2972.5 & 446500 & 2.1555d7 \end{pmatrix}. \tag{9}$$

The BAO measurements considered in our analysis are obtained from three aspects of observations. The first is the A parameter measured at three redshifts

[a]Point mass is not a realistic model to characterize the mass profile for extra lenses. However, in PixeLens it just allows local spikes in the pixelated mass map which can override the nearest neighbor constraint.

$z = 0.44$, $z = 0.6$ and $z = 0.73$ from WiggleZ dark energy survey.[58,59] The second is the BAO distance ratio d_z at $z = 0.2$, $z = 0.35$ from SDSS data release 7 (DR7) galaxy sample,[60,82,83] and $z = 0.106$ from the 6dFGS measurements.[58] The third is the direct measurement the value of $\theta_{\rm BAO}(z = 0.55) = (3.90 \pm 0.38)^\circ$ for the angular BAO scale including systematic errors.[84] The definition of $\theta_{\rm BAO}$ expresses as

$$\theta_{\rm BAO} = \frac{r_s(z_d)}{d_L(z)}, \tag{10}$$

where the comoving radial distance $d_L(z)$ depending on model is defined as

$$d_L(z) = \frac{1}{H_0}\int_0^z \frac{dz}{E(a)}. \tag{11}$$

For the SN Ia data, following the statistical method based on the moduli distance,[55,85] we use the Union2.1 compilation which consists of 580 SN Ia.[80] For each of these observational tests we evaluate the fitting function χ^2, and the model parameters $\mathbf{p}$ are determined by applying the maximum likelihood method of χ^2 fit. In the MCMC approach, a chain of sample points is generated in the parameter space according to the posterior probability (we use the Metropolis–Hastings algorithm with uniform prior probability distribution), which is repeated until the established convergence accuracy can be satisfied. Our code is based on CosmoMC[86] and we generated eight chains to guarantee the accuracy of this work.

3. Models and Constraining Results

In view of continuity equations, the interaction between DE and DM must be a function of the energy density multiplied by a quantity with units of inverse of time, which can be chosen as the Hubble factor H. By choosing different forms of the energy densities, the simplest expressions for the interaction term are[47,48,87]

$$Q_1 = 3\gamma_m H\rho_m \tag{12}$$

and[48]

$$Q_2 = 3\gamma_x H\rho_X, \tag{13}$$

where the constants γ_m and γ_x quantify the extent of interaction between dust matter and DE. Another interaction with only one parameter can be obtained from the phenomenological assumption on the ratio of the DE and matter densities $\frac{\rho_X}{\rho_m} = \frac{\rho_{X0}}{\rho_{m0}}a^\xi$,[46] where ξ is a constant parameter quantifying the severity of the coincidence problem. Considering a flat FRW universe, it is easy to find that the corresponding interaction term Q can be given by Dalal *et al.*[46] and Guo *et al.*[44,46]

$$Q_3 = \frac{-(1-\Omega_m)(\xi + 3w_x)}{1-\Omega_m+\Omega_m(1+z)^\xi}H\rho_m, \tag{14}$$

where Ω_m is the present value of density parameter of dust matter. We assume that, for the three phenomenological interaction models, the EoS of dark energy $w_x \equiv p/\rho$ is a constant in spatially flat FRW metric. In this paper, we adopt the simple models with constant exchange terms γ_m, γ_x and the phenomenological form $\rho_X \propto \rho_m a^{\xi}$, where γ_m, γ_x and ξ denote the severity of the coincidence problem. In the three cases, the standard cosmology without interaction between DE and DM is characterized by $\gamma_m = 0$, $\gamma_x = 0$ and $\xi + 3w_x = 0$, while $\gamma_m \neq 0$, $\gamma_x \neq 0$ and $\xi + 3w_x \neq 0$ denote nonstandard cosmology. For the first two models, the special cases ($w_x = -1$, $\gamma_m = 0$ ($\gamma_x = 0$)) correspond to ΛCDM; while for the third one, the special cases $\xi = 3$ and $\xi = 0$ correspond to ΛCDM and the self-similar solution without coincidence problem respectively, and thus any solution with a scaling parameter $0 < \xi < 3$ makes the coincidence problem less severe.[88] Furthermore, $\gamma_m < 0$ or $\gamma_x < 0$, corresponding to $\xi + 3w_x > 0$, indicates that the energy is transferred from DM to DE. On the other hand, $\gamma_m > 0$ or $\gamma_x > 0$, corresponding to $\xi + 3w_x < 0$, denotes that the energy is transferred from DE to DM. The values of γ_m and γ_x determine the extent of interaction and transfer direction between DE and DM; while from the value of ξ, we can understand how severe the coincidence problem is. In this paper, in order to set stringent limit on the matter density parameter Ω_m, the CMB + BAO data are taken as priors and combined with other data to test the constraining power of TDD data. Thus, we will constrain three interaction dark sectors and sample the parameters with $D_{\Delta t}$ + SN + CMB + BAO, SN + CMB + BAO, and $D_{\Delta t}$ + CMB + BAO, respectively. In the following, we will treat the three cases separately and the best-fit parameters (with 1σ uncertainties) for the three interacting DE scenarios are presented in Table 1.

3.1. *The γ_mIDE model*

When the interaction between the DE and DM takes the form $Q_1 = 3\gamma_m H\rho_m$, we can obtain the Hubble parameter

$$E^2(z) = \frac{w_x\Omega_m}{\gamma_m + w_x}(1+z)^{3(1-\gamma_m)} + \left(1 - \frac{w_x\Omega_m}{\gamma_m + w_x}\right)(1+z)^{3(1+w_x)}, \qquad (15)$$

where $\Omega_m = 8\pi G\rho_{m0}/(3H_0^2)$ is the present fractional energy density of dust matter. The free parameters are H_0, Ω_m, w_x and γ_m. In the first step, the Hubble constant H_0 is determined by minimizing the three-dimensional χ^2 function. The remaining parameters then are Ω_m, w_x and γ_m, for which we perform the statistical analysis. The results are displayed in Fig. 1.

When constrained by $D_{\Delta t}$ + SN + CMB + BAO, the best-fit value for the parameters are $\Omega_m = 0.291^{+0.014}_{-0.013}$, $w_x = -1.016^{+0.036}_{-0.035}$, and $\gamma_m = 0.001^{+0.002}_{-0.002}$ at 68.3% confidence level. The marginalized 2D confidence contours of parameters (w_x and γ_m, w_x and $\Omega_{\rm m}$, γ_m and $\Omega_{\rm m}$) are shown in Fig. 1. Although the best-fit interaction term between DE and DM is slightly larger than zero, which suggests that the energy is transferred from DE to DM and the coincidence problem is relatively

Table 1. The best-fit values (with the 1σ uncertainties) of the parameters in three IDE models with different data combinations, all represents $D_{\Delta t}$+SN+BAO+CMB, all-$D_{\Delta t}$ represents SN + BAO + CMB, all-SN means $D_{\Delta t}$ + BAO + CMB, and BAO + CMB are the priors.

	The γ_mIDE Model		
	$\Omega_{\rm m}$	w_x	γ_m
all	$0.291^{+0.014}_{-0.013}(1\sigma)$	$-1.016^{+0.036}_{-0.035}(1\sigma)$	$0.001^{+0.002}_{-0.002}(1\sigma)$
all-$D_{\Delta t}$	$0.292^{+0.014}_{-0.014}(1\sigma)$	$-1.022^{+0.036}_{-0.036}(1\sigma)$	$0.001^{+0.002}_{-0.002}(1\sigma)$
all-SN	$0.303^{+0.019}_{-0.019}(1\sigma)$	$-0.971^{+0.037}_{-0.038}(1\sigma)$	$0.0006^{+0.0028}_{-0.0029}(1\sigma)$
priors	$0.302^{+0.018}_{-0.018}(1\sigma)$	$-0.980^{+0.038}_{-0.039}(1\sigma)$	$0.0009^{+0.0028}_{-0.0028}(1\sigma)$
	The γ_xIDE Model		
	$\Omega_{\rm m}$	w_x	γ_x
all	$0.300^{+0.006}_{-0.007}(1\sigma)$	$-1.040^{+0.065}_{-0.065}(1\sigma)$	$-0.004^{+0.011}_{-0.011}(1\sigma)$
all-$D_{\Delta t}$	$0.302^{+0.006}_{-0.009}(1\sigma)$	$-1.066^{+0.068}_{-0.069}(1\sigma)$	$-0.008^{+0.011}_{-0.012}(1\sigma)$
all-SN	$0.302^{+0.01}_{-0.01}(1\sigma)$	$-0.954^{+0.081}_{-0.081}(1\sigma)$	$0.003^{+0.013}_{-0.013}(1\sigma)$
priors	$0.308^{+0.010}_{-0.011}(1\sigma)$	$-1.007^{+0.099}_{-0.096}(1\sigma)$	$-0.005^{+0.016}_{-0.015}(1\sigma)$
	The ξIDE Model		
	$\Omega_{\rm m}$	w_x	ξ
all	$0.299^{+0.007}_{-0.007}(1\sigma)$	$-1.038^{+0.063}_{-0.063}(1\sigma)$	$3.136^{+0.245}_{-0.245}(1\sigma)$
all-$D_{\Delta t}$	$0.302^{+0.007}_{-0.007}(1\sigma)$	$-1.063^{+0.067}_{-0.097}(1\sigma)$	$3.235^{+0.260}_{-0.261}(1\sigma)$
all-SN	$0.302^{+0.01}_{-0.01}(1\sigma)$	$-0.956^{+0.079}_{-0.078}(1\sigma)$	$2.847^{+0.306}_{-0.308}(1\sigma)$
priors	$0.307^{+0.011}_{-0.01}(1\sigma)$	$-1.002^{+0.094}_{-0.094}(1\sigma)$	$3.028^{+0.365}_{-0.367}(1\sigma)$

alleviated, a nonzero coupling between dark sectors ($\gamma_m = 0$) is still included within 1σ confidence region. This is noted by using the 182 Gold SNIa together with CMB and large-scale structure for the interacting holographic DE model[43] and by using the revised Hubble parameter data together with CMB and BAO.[85]

In order to illustrate the impact of SGL data, we also show the cosmological constraints from the combination of SN+BAO+CMB without $D_{\Delta t}$ and $D_{\Delta t}$ + CMB+BAO without SN in Fig. 1. Fitting results from the BAO+CMB data, which play a prior role in all data combinations, are also plotted with dotted contours. It is obvious that the current strong lensing data are consistent with other observations, although they give larger errors and contribute little to the combined constraints. Meanwhile, when comparing the constraints obtained with and without SGL data, we see that the degeneracies between Ω_m and w_x, w_x and γ_m are different; as for the best-fit parameters, the interaction term γ_m is shifted to a smaller value when SGL data are added to combined analysis, while Ω_m and w_x are driven to larger values. Considering they are only 10% of the whole data set in this work, the SGL data do not shift the best-fit significantly. However, in the other two following models, we can find the non-negligible effect of the SGL data on the parameter constraints.

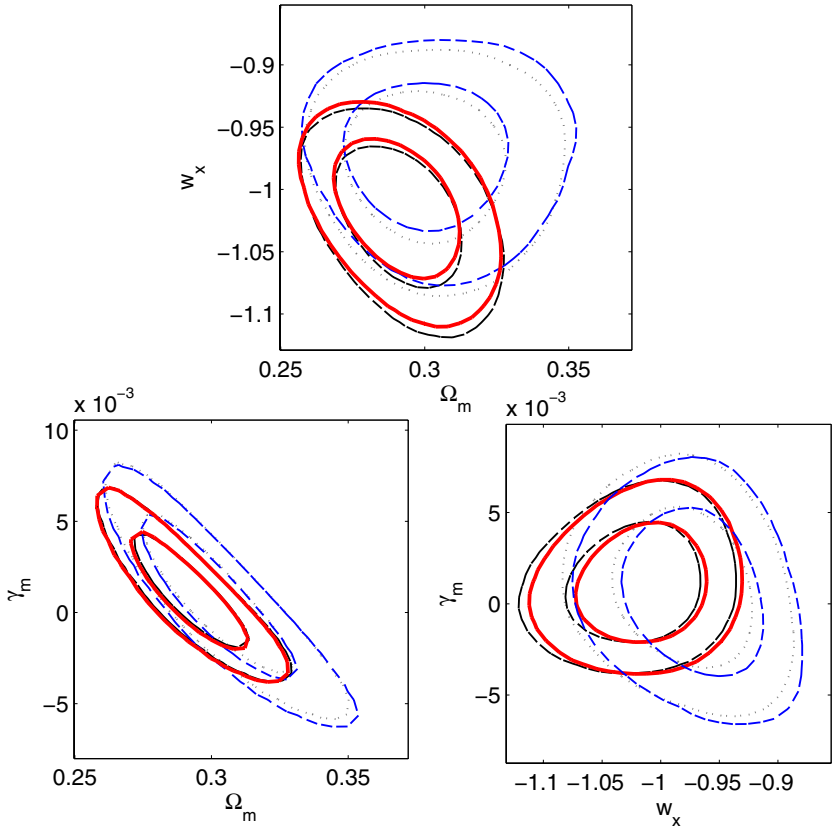

Fig. 1. (Color online) The 2D regions with the 2σ contours of parameters w_x and γ_m, Ω_m and γ_m, Ω_m and w_x in the γ_mIDE model. The BAO + CMB priors are shown in gray dotted line, the red line represents the fits from $D_{\Delta t}$ + BAO + CMB + SN, the black dashed line represent those from SN + BAO + CMB, and the blue dashed line represent those from $D_{\Delta t}$ + BAO + CMB.

3.2. *The γ_xIDE model*

Performing a similar analysis as before, this time with the interaction proportional to the DE density $Q_2 = 3\gamma_x H\rho_X$, we obtain the Hubble parameter

$$E^2(z) = (1-\Omega_m)(1+z)^{3(1+\gamma_x+w_x)} + \frac{w_x\Omega_m + \gamma_x + \gamma_x(\Omega_m - 1)(1+z)^{3(\gamma_x+w_x)}}{(1+z)^{-3}(w_x+\gamma_x)}. \tag{16}$$

By minimizing the total $\chi^2_{\rm total}$, the matter density implied by our statistical analysis gives $\Omega_m = 0.300^{+0.006}_{-0.007}$. The best-fit obtained for the DE parameters are $w_x = -1.040^{+0.065}_{-0.065}$ and $\gamma_x = -0.004^{+0.011}_{-0.011}$ (68.3% confidence level). The best-fit value of γ_x indicates that the energy is transferred from DE to DM and the coincidence problem is not alleviated. The small negative coupling provided by joint analysis agrees with the results by using the Gold SNIa together with CMB

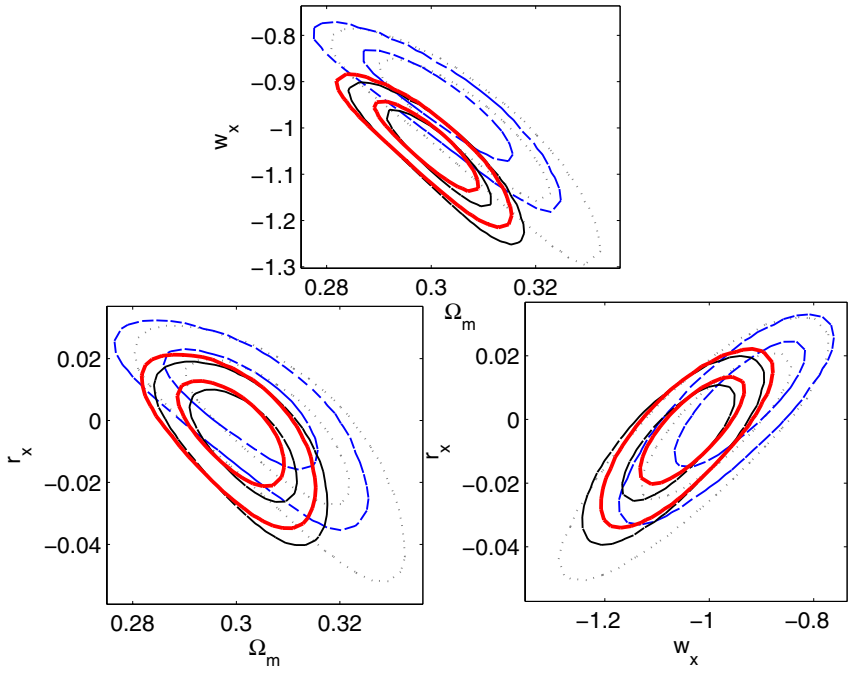

Fig. 2. The same as Fig. 1, but for the γ_xIDE model.

and large-scale structure for other interacting DE models describing the interaction in proportional to the DM energy density.[44] In order to check the impact of SGL data points, confidence contours from SN + BAO + CMB without $D_{\Delta t}$ and $D_{\Delta t}$ + BAO + CMB without SN are also plotted in Fig. 2. We note that compared to the constraint with SN, the gravitational lenses shift the best-fit to a larger value for the dark energy EoS parameter w_x and a positive coupling between DE and DM ($\gamma_x = 0.003^{+0.013}_{-0.013}$ with $D_{\Delta t}$ + BAO + CMB). In addition, the constraining results in this work with joint observational data including $D_{\Delta t}$ are essentially the same in comparison to the results of Cao *et al.* (2013),[85] which incorporate combined observations including the 28 $H(z)$ measurements from the differential ages of red-envelope galaxies as well as the BAO peaks. However, we remark here that, from Fig. 2 and Table 1, ΛCDM ($\gamma_x = 0$) is still included within 1σ confidence region.

3.3. *The ξIDE model*

In the ξIDE model, the interaction between DM and DE is given by $Q_3 = \frac{-(1-\Omega_m)(\xi+3w_x)}{1-\Omega_m+\Omega_m(1+z)^{\xi}} H\rho_m$, and the corresponding Hubble parameter now has the form

$$E^2(z) = (1+z)^3[\Omega_m + (1-\Omega_m)(1+z)^{-\xi}]^{-3w_x/\xi}. \tag{17}$$

We show the contours constrained from the joint analysis in Fig. 3 and the best-fit is $\Omega_m = 0.299^{+0.007}_{-0.007}$, $w_x = -1.038^{+0.063}_{-0.063}$ and $\xi = 3.136^{+0.245}_{-0.245}$ (68.3%

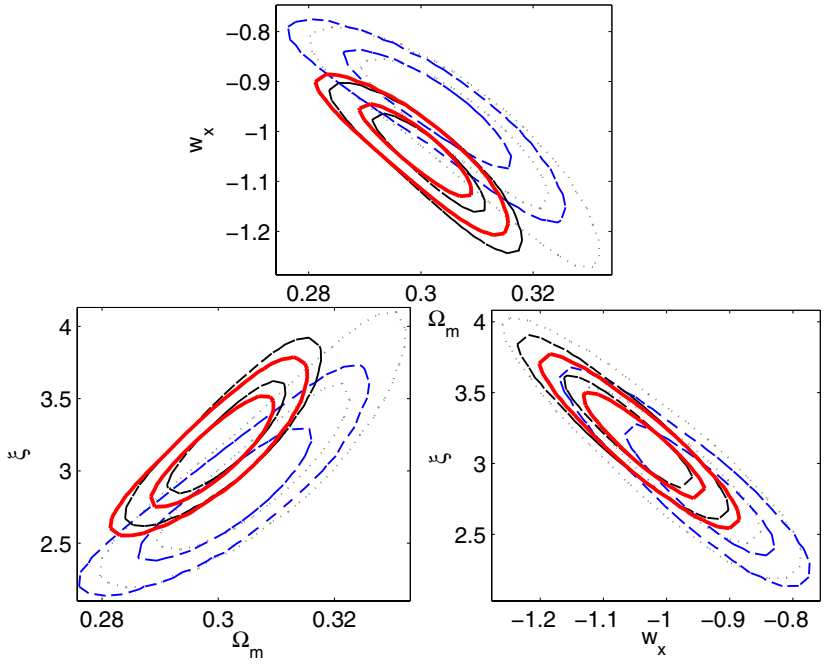

Fig. 3. The same as Fig. 1, but for the ξIDE model.

confidence level). Obviously, the combined data contours including the SGL data are shifted compared to those without them, which also demonstrates the non-negligible effect of the strong lensing data on model constraints. Following the other two models, another parameter $\gamma = -(\xi + 3w_x)$ is introduced to test the energy transfer direction between DE and DM. The best-fit value for this interaction term is $\gamma = -0.022^{+0.056}_{-0.056}$. Evidently, a negative value for the interaction is still favored in the framework of this relatively complicated ξIDE model. The significant effect of the SGL data should also be pointed out: both Ω_m and w_x are shifted to larger values when SGL data are added to combined analysis ($\Omega_m = 0.302^{+0.01}_{-0.01}$, $w_x = -0.956^{+0.079}_{-0.078}$). Moreover, we infer the best-fit of γ to be $\gamma = -0.021$ from $D_{\Delta t}$ + BAO + CMB.

Meanwhile, the ΛCDM model is still supported within 1σ error region, which is consistent with the constraint result obtained by using the Constitution Set (397 SN Ia data) together with the CMB shift parameter from the five-year WMAP and the SDSS baryon acoustic peak,[54] and by using the observational $H(z)$ data together with the CMB observation from the WMAP7 results and the BAO observation from the SDSS7 data release.[55] However, compared with the results obtained in the previous analysis,[54] $\Omega_m = 0.28 \pm 0.02$, $w_X = -0.98 \pm 0.07$ and $\xi = 3.06 \pm 0.35$, the shift in the best-fitted parameters (with remarkably reduced allowed region) illustrates how the combination of the most recent cosmological observations (including the

time delay measurements from SGL) can be used to probe the interaction between DM and DE.

4. Analysis

In this section, we will use the information criteria (IC) to compare the three interacting DE models, check the consistency between SGL data and models with best-fit parameters, and test the coincidence problem concerning the change of DE and matter densities with redshifts.

Based on a likelihood method, one may employ the IC to assess different models. In this paper, we will apply the Akaike Information Criteria (AIC),[89] Bayesian Information Criteria (BIC),[90] and Kullback Information Criterion (KIC)[91] as model selection criteria. According to these criteria, models that give a good fit with fewer parameters will be more favored. The application of the BIC, AIC and KIC in a cosmological context can be found in the previous study.[53,92–94]

The BIC is given by

$$\mathrm{BIC} = -2\ln\mathcal{L}_{\max} + k\ln N, \tag{18}$$

the AIC is defined as

$$\mathrm{AIC} = -2\ln\mathcal{L}_{\max} + 2k, \tag{19}$$

and the KIC is defined as

$$\mathrm{KIC} = -2\ln\mathcal{L}_{\max} + 3k, \tag{20}$$

where $\mathcal{L}_{\max}$ is the maximum likelihood, k is the number of parameters, and N is the number of data points. Note that for Gaussian errors, $\chi^2_{\min} = -2\ln\mathcal{L}_{\max}$. we obtain $\chi^2_{\min}$ and calculate their corresponding AIC, BIC and KIC values shown in Table 2.

In the one-on-one model comparison, model M_α with characterizing IC_α has the likelihood[27]

$$P(M_\alpha) = \frac{\exp\left(-\frac{\mathrm{IC}_\alpha}{2}\right)}{\exp\left(-\frac{\mathrm{IC}_1}{2}\right) + \exp\left(-\frac{\mathrm{IC}_2}{2}\right)}, \tag{21}$$

of being the correct choice, and the difference $\Delta\mathrm{IC} = \mathrm{IC}_2 - \mathrm{IC}_1$ determines the extent to which M_1 is favored over M_2.[89–91] Taking the comparison between γ_mIDE and

Table 2. The IC values for the three models considered in this analysis.

IC	γ_mIDE model	γ_xIDE model	ξIDE model
$\chi^2_{\min}$	584.72	585.02	585.02
BIC	610.36	610.66	610.66
AIC	592.72	593.02	593.02
KIC	596.72	597.02	597.02

γ_xIDE for instance, for all three types of IC we find the likelihood of γ_mIDE being a better model is $P(M_1) \approx 53\%$–54%, while the corresponding value for γ_xIDE is $P(M_2) \approx 46\%$–47%, which indicates that γ_mIDE is favored over r_dIDE by a likelihood of $\approx 53\%$–54% versus 46%–47%. Similar results could also be obtained from the comparison between γ_xIDE and ξIDE model.

Moreover, since the γ_mIDE model gives better constraint among the three interaction DE models, with the best-fit parameters from $D_{\Delta t}$+BAO+CMB+SN, we obtain the theoretical values of TDD data and compare them with the corresponding observations. The 3D plot among redshifts of lens, redshifts of source and TDD is shown in Fig. 4. We can clearly see the agreement between the theoretical and values and observations. In fact, in the past decades, separate investigations with standard rulers have been made specially to carry out geometric tests of cosmological models, based on the redshift — angular size relation for different types of sources.[95,96] From our analysis, time delay lenses could introduce another standard ruler with systematics different from other cosmological probes, thus providing a complementary tool to check the results obtained from other important tests above.

Finally, we discuss the ratio r between ρ_m and ρ_X to analyze the coincidence problem. If the ratio $r = \rho_m/\rho_X$ does not change much during the whole history of the universe, the coincidence problem can be alleviated. By combining Eq. (2), we obtain the ratio r evolving as[97]

$$\dot{r} = 3Hr(1+r)\left[\frac{w_x}{1+r} + \frac{Q}{3H\rho_m}\right], \tag{22}$$

where Q is the interaction term of the three interacting DE models. In Fig. 5, we show the evolution of the ratio as a function of redshifts for the best-fit values from

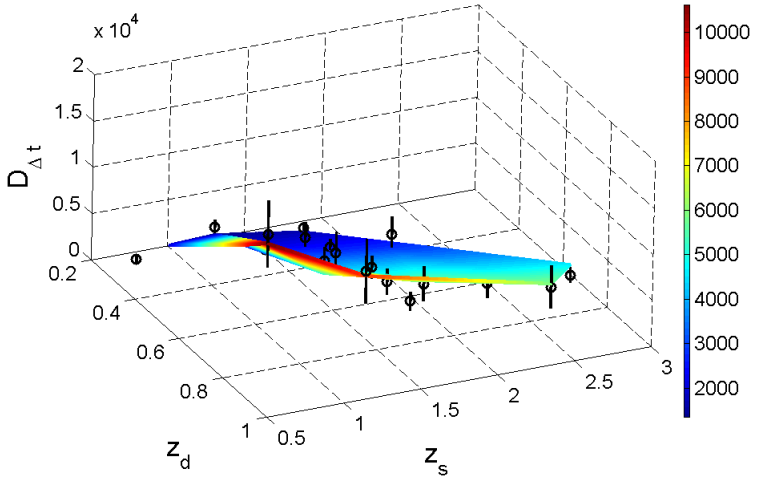

Fig. 4. 3D Hubble diagram distribution of the 18 strong lensing systems. X-axis is the lens redshift, Y is the redshift of the source, and Z is the time delay distance $D_{\Delta t}$. The reference surface corresponds to our best-fit γ_mIDE model ($D_{\Delta t}$ + BAO + CMB + SN). Black circles with error bars represent the observational time delay distance data.

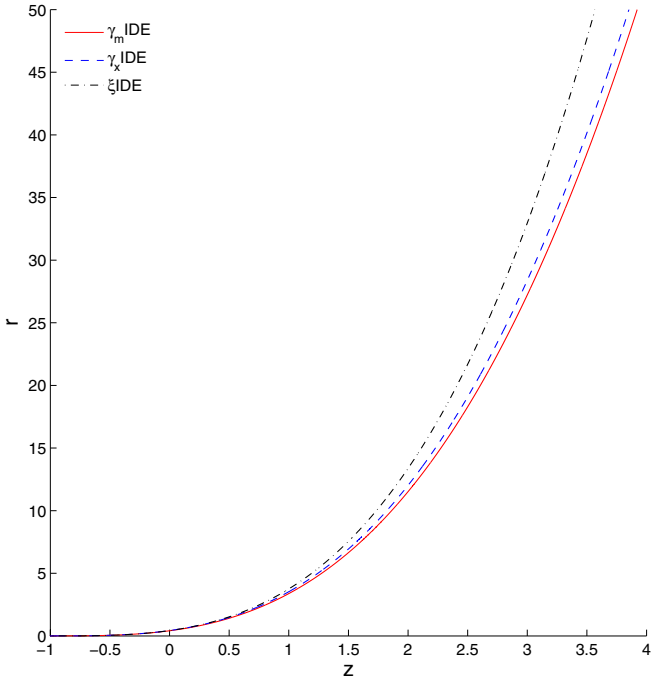

Fig. 5. The evolution of the ratio r as a function of z in γ_mIDE, γ_xIDE, ξIDE models. The model parameters are taken as the best-fit values from $D_{\Delta t}$ + SN + BAO + CMB.

the joint data of $D_{\Delta t}$, SN, BAO and CMB. In particular, we find that far away from $z = 2.0$ the universe is dominated by the matter, while nearly close to $z = 0$, the DE controls the dynamic of the universe and fuels the cosmic acceleration.

5. Conclusion

In this paper, we have used the measurements of the TDD between multiple images of 18 strongly lensed systems, to provide additional constraints on three interacting DE models, which allow the possibility for a continuous energy transfer between the DM and the unknown DE fluid. These models either introduce an energy transfer Q proportional to the matter density ($\propto \gamma_m \rho_{\rm m}$), to the DE density ($\propto \gamma_x \rho_{\rm x}$), or assume that the ratio of the DE density to matter density is a power-law function of the cosmological scaling factor ($\frac{\rho_{\rm x}}{\rho_{\rm m}} \propto a^{\xi}$).

Firstly, we find that the interaction term between DE and DM still seems to be of a small value close to zero, which is compatible with the previous results for constraining interacting DE parameters. We also note that the interaction parameter is correlated with other model parameters Ω_m and w_x, and the concordance ΛCDM model with $\gamma = 0$ is within the 1σ confidence region. More importantly, the current strong lensing data, which are consistent with other observations including SN, may shift the best-fit interaction term γ_x to a positive value in the γ_xIDE model and

significantly lead to a larger value for the dark energy EoS parameter w_x for all three IDE models. Considering the SGL data take up only 10% of the whole data set, the time delay distance method has the potential to tighten the constraint on the parameters with future larger sample.

Secondly, we have also provided three types of IC results for each model in Table 2. Compared with the other two γ_xIDE and ξIDE models, the γ_mIDE model provides relatively better fits to recent observations. However, the coincidence problem is still very severe in the framework of three interacting DE models, since the fitting results does not show any preference for a nonzero coupling between DM and DE.

Finally, considering that 1000s of lensed quasars will be discovered by wide field imaging surveys within the next decade, our results highlight the importance of strong lensing time delay measurements (see Fig. 4) to provide additional observational fits on alternative cosmological models, which are necessary to derive the information of the interaction between dark sectors in the dark universe. We also hope future observational data including high redshift SNeIa from SDSS-II and SNLS collaborations[98] and weak lensing survey (like EUCLID) combined CMB measurements[56] may improve remarkably the constraints on the coupling parameters.

Acknowledgments

This work was supported by the Ministry of Science and Technology National Basic Science Program (Project 973) under Grants Nos. 2012CB821804 and 2014CB845806, the National Natural Science Foundation of China under Grants Nos. 11503001, 11073005, 11005164, 11373014 and 11447213, the Scientific and Technological Research Program of Chongqing Municipal Education Commission (Grant No. KJ130535), and the Scientific Research Foundation For Doctor of Chongqing University of Posts and Telecommunications (Nos. A2013-25 and A2014-43). Cao S. also thanks the support from the Fundamental Research Funds for the Central Universities and Scientific Research Foundation of Beijing Normal University, and China Postdoctoral Science Foundation under Grant Nos. 2014M550642 and 2015T80052.

References

1. D. Walsh *et al.*, *Nature* **279** (1979) 381.
2. Z.-H. Zhu, *Int. J. Mod. Phys. D* **9** (2000) 591.
3. K.-H. Chae, *Mon. Not. R. Astron. Soc.* **346** (2003) 746.
4. K.-H. Chae *et al.*, *Astrophys. J.* **607** (2004) L71.
5. J. L. Mitchell *et al.*, *Astrophys. J.* **622** (2005) 81.
6. Z.-H. Zhu *et al.*, *Astron. Astrophys.* **487** (2008) 831.
7. S. Cao *et al.*, *J. Cosmol. Astropart. Phys.* **03** (2012) 016.
8. S. Cao *et al.*, *Astrophys. J.* **755** (2012) 31.
9. S. Cao *et al.*, *Phys. Rev. D* **90** (2014) 083006.

10. A. Einstein, *Ann. Phys.* **343** (1912) 1059.
11. P. Schneider, J. Ehlers and E. E. Falco, *Gravitational Lenses* (Springer-Verlag, Berlin, 1992).
12. S. Refsdal, *Mon. Not. R. Astron. Soc.* **128** (1964) 307.
13. D. Coe and L. A. Moustakas, *Astrophys. J.* **706** (2009) 45.
14. S. H. Suyu *et al.*, *Astrophys. J.* **788** (2014) L35.
15. A. Eigenbrod *et al.*, *Astron. Astrophys.* **436** (2005) 25.
16. C. Jean *et al.*, Gravitational lensing: Recent progress and future goals, *ASP Conf. Proc.*, Vol. 237, eds. T. G. Brainerd and C. S. Kochanek (ASP: San Franciso, 2001).
17. M. Banerji *et al.*, *Mon. Not. R. Astron. Soc.* **386** (2008) 1219.
18. E. J. Buckley-Geer *et al.*, *AAS Meet.* **223** (2014) 248.01.
19. M. D. Schneider, *Phys. Rev. Lett.* **112** (2014) 061301.
20. C. S. Kochanek *et al.*, Part 2 of Gravitational lensing: Strong, weak and Micro, *Proc. 33rd Saas-Fee Advanced Course*, eds. G. Meylan, P. Jetzer and P. North (Springer-Verlag: Berlin, 2004).
21. E. V. Linder, *Phys. Rev. D* **84** (2011) 123529.
22. T. Treu *et al.*, arXiv:1306.1272.
23. S. Mauro *et al.*, *Mon. Not. R. Astron. Soc.* **473** (2013) 1.
24. P. Saha *et al.*, *Astrophys. J.* **650** (2006) L17.
25. J. Coles, *Astrophys. J.* **679** (2008) 17.
26. D. Paraficz *et al.*, *Astrophys. J.* **712** (2010) 1378.
27. J. J. Wei *et al.*, arXiv:1405.2388v1.
28. A. G. Riess *et al.*, *Astron. J.* **116** (1998) 1009.
29. S. Perlmutter *et al.*, *Astrophys. J.* **517** (1999) 565.
30. A. G. Riess *et al.*, *Astron. J.* **607** (2004) 665.
31. R. A. Knop *et al.*, *Astron. J.* **598** (2007) 102.
32. A. Balbi *et al.*, *Astron. J.* **545** (2000) L1.
33. A. H. Jaffe *et al.*, *Phys. Rev. Lett.* **86** (2001) 3475.
34. D. N. Spergel *et al.*, *Astrophys. J. Suppl.* **148** (2003) 175.
35. D. N. Spergel *et al.*, *Astrophys. J. Suppl.* **170** (2007) 377.
36. C. Wetterich, *Nucl. Phys. B* **302** (1988) 668.
37. W. Zimdahl, D. Pavn and L. P. Chimento, *Phys. Lett. B* **521** (2001) 133.
38. Y. L. Bolotin, A. Kostenko, O. A. Lemets and D. A. Yerokhin, *Int. J. Mod. Phys. D* **24** (2015) 1530007.
39. L. Amendola, *Phys. Rev. D* **62** (2000) 043511.
40. G. Olivares *et al.*, *Phys. Rev. D* **74** (2006).
41. B. Wang *et al.*, *Phys. Lett. B* **624** (2005) 141.
42. B. Wang *et al.*, *Nucl. Phys. B* **778** (2007) 69.
43. C. Feng *et al.*, *J. Cosmol. Astropart. Phys.* **09** (2007) 005.
44. Z. K. Guo *et al.*, *Phys. Rev. D* **76** (2007) 023508.
45. O. Bertolami *et al.*, *Phys. Lett. B* **654** (2007) 165.
46. N. Dalal *et al.*, *Phys. Rev. Lett.* **87** (2001) 141302.
47. H. Wei *et al.*, *Phys. Lett. B* **644** (2007) 7.
48. Y. Zhang *et al.*, *J. Cosmol. Astropart. Phys.* **1006** (2010) 003.
49. E. J. Copeland *et al.*, *Phys. Rev. D* **57** (1998) 4686.
50. L. P. Chimento *et al.*, *Phys. Rev. D* **67** (2003) 083513.
51. R. G. Cai *et al.*, *J. Cosmol. Astropart. Phys.* **0503** (2005) 002.
52. S. Nojiri *et al.*, *Phys. Rev. D* **72** (2005) 023003.
53. M. Szydlowski, *Phys. Lett. B* **632** (2006) 1.
54. Y. Chen *et al.*, *Astrophys. J.* **711** (2010) 439.

55. S. Cao *et al.*, *Mon. Not. R. Astron. Soc.* **416** (2011) 1099.
56. P. A. R. Ade *et al.*, arXiv:1303.5076.
57. Y. Wang *et al.*, *Phys. Rev. D* **88** (2013) 043522.
58. C. Blake *et al.*, *Mon. Not. R. Astron. Soc.* **418** (2011) 1707.
59. Y. Gong and Q. Gao, arXiv:1301.1224.
60. W. J. Percival *et al.*, *Mon. Not. R. Astron. Soc.* **401** (2010) 2148.
61. C. R. Keeton *et al.*, *Astrophys. J.* **598** (2003) 138.
62. S. J. Warren *et al.*, *Astrophys. J.* **590** (2003) 673.
63. M. Bradac *et al.*, *Astrophys. J.* **687** (2008) 959.
64. S. H. Suyu *et al.*, *Astrophys. J.* **766** (2013) 70.
65. S. H. Suyu *et al.*, *Astrophys. J.* **711** (2010) 201.
66. S. Vegetti *et al.*, *Mon. Not. R. Astron. Soc.* **408** (2010) 1969.
67. P. Saha *et al.*, *Astron. J.* **127** (2004) 2604.
68. M. Sereno and D. Paraficz, *Mon. Not. R. Astron. Soc.* **437** (2014) 600.
69. E. Eulaers *et al.*, *Astron. Astrophys.* **536** (2011) A53.
70. L. J. Goicoechea *et al.*, *New A.* **13** (2008) 182.
71. A. Ullan *et al.*, *Astron. Astrophys.* **452** (2006) 25.
72. A. Oscoz *et al.*, *Astrophys. J.* **552** (2001) 81.
73. E. Eulaers *et al.*, *Astron. Astrophys.* **553** (2013) A121.
74. C. Vuissoz *et al.*, *Astron. Astrophys.* **464** (2007) 845.
75. J. E. J. Lovell *et al.*, *Astrophys. J.* **508** (1998) L51.
76. J. Fohlmeister *et al.*, *Astrophys. J.* **676** (2008) 761.
77. M. Tewes *et al.*, arXiv:1208.6009.
78. C. Vuissoz *et al.*, *Astron. Astrophys.* **488** (2008) 481.
79. F. Courbin *et al.*, *Astron. Astrophys.* **536** (2011) A53.
80. N. Suzuki *et al.*, *Astrophys. J.* **746** (2012) 85.
81. WMAP Collab. (E. Komatsu *et al.*), arXiv:1001.4538.
82. D. Eisenstein *et al.*, *Astrophys. J.* **633** (2005) 560.
83. D. Eisenstein *et al.*, *Astrophys. J.* **496** (1998) 605.
84. M. Crocce *et al.*, *Mon. Not. R. Astron. Soc.* **417** (2011) 2577.
85. S. Cao *et al.*, *Int. J. Mod. Phys. D* **22** (2013) 1350082.
86. A. Lewis *et al.*, *Phys. Rev. D* **66** (2002) 103.
87. H. Wei *et al.*, *Phys. Lett. B* **654** (2007) 139.
88. D. Pavon *et al.*, *J. Cosmol. Astropart. Phys.* **0405** (2004) 009.
89. G. Schwarz, *Ann. Stat.* **6** (1978) 461.
90. H. Akaike, *IEEE Trans. Autom. Control* **19** (1974) 716.
91. J. E. Cavanaugh, *Aust. N. Z. J. Stat.* **46** (2004) 257.
92. A. R. Liddle, *Mon. Not. R. Astron. Soc.* **315** (2004) L49.
93. M. Biesiada, *J. Cosmol. Astropart. Phys.* **0702** (2007) 003.
94. S. Cao *et al.*, *Phys. Rev. D* **84** (2011) 023005.
95. R. A. Daly *et al.*, *Astrophys. J.* **597** (2003) 9.
96. S. Cao *et al.*, *Astrophys. J.* **806** (2015) 66.
97. L. P. Chimento *et al.*, *Phys. Rev. D* **63** (2001) 103508.
98. M. Betoule *et al.*, arXiv:1401.4064.